MOLECULAR AND CELLULAR BIOLOGY, June 2011, p. 2369–2379 Vol. 31, No. 12
0270-7306/11/$12.00 doi:10.1128/MCB.05312-11

Phenotypes in *mTERT*$^{+/-}$ and *mTERT*$^{-/-}$ Mice Are Due to Short Telomeres, Not Telomere-Independent Functions of Telomerase Reverse Transcriptase▽‡

Margaret A. Strong,[1]† Sofia L. Vidal-Cardenas,[1]† Baktiar Karim,[2] Huimin Yu,[1] Nini Guo,[1] and Carol W. Greider[1]*

Department of Molecular Biology & Genetics[1] *and Department of Molecular & Comparative Pathobiology,*[2] *The Johns Hopkins University School of Medicine, Baltimore, Maryland*

Received 7 March 2011/Returned for modification 15 March 2011/Accepted 23 March 2011

Telomerase is essential for telomere length maintenance. Mutations in either of the two core components of telomerase, telomerase RNA (TR) or the catalytic protein component telomerase reverse transcriptase (TERT), cause the genetic disorders dyskeratosis congenita, pulmonary fibrosis, and other degenerative diseases. Overexpression of the TERT protein has been reported to have telomere length-independent roles, including regulation of the Wnt signaling pathway. To examine the phenotypes of TERT haploinsufficiency and determine whether loss of function of TERT has effects other than those associated with telomere shortening, we characterized both *mTERT*$^{+/-}$ and *mTERT*$^{-/-}$ mice on the CAST/EiJ genetic background. Phenotypic analysis showed a loss of tissue renewal capacity with progressive breeding of heterozygous mice that was indistinguishable from that of *mTR*-deficient mice. *mTERT*$^{-/-}$ mice, from heterozygous *mTERT*$^{+/-}$ mouse crosses, were born at the expected Mendelian ratio (26.5%; $n = 1{,}080$ pups), indicating no embryonic lethality of this genotype. We looked for, and failed to find, hallmarks of Wnt deficiency in various adult and embryonic tissues, including those of the lungs, kidneys, brain, and skeleton. Finally, *mTERT*$^{-/-}$ cells showed wild-type levels of Wnt signaling *in vitro*. Thus, while TERT overexpression in some settings may activate the Wnt pathway, loss of function in a physiological setting has no apparent effects on Wnt signaling. Our results indicate that both TERT and TR are haploinsufficient and that their deficiency leads to telomere shortening, which limits tissue renewal. Our studies imply that hypomorphic loss-of-function alleles of *hTERT* and *hTR* should cause a similar disease spectrum in humans.

Short telomeres play a critical role in human disease. It was first shown that short telomeres underlie the bone marrow failure seen in autosomal dominant dyskeratosis congenita (57, 72). Short telomeres are also associated with a broad spectrum of degenerative disorders that are linked to aging, including aplastic anemia, pulmonary fibrosis, liver disease, and others (1, 4, 5, 11, 41, 70, 78, 79). While these diseases were once thought to be distinct, it is now clear that they share the common molecular defect of progressive telomere shortening (2). Progressive telomere shortening generates critically short telomeres that limit the replicative capacity of cells (30) and, in mice, is known to cause loss of tissue renewal capacity (29, 42) and progressive organ failure (2).

Telomeres cap chromosome ends and distinguish a natural chromosome end from a DNA break. When telomeres become critically short, the protective function is lost, initiating a DNA damage response (18, 20, 36). This damage response signals through p53, leading to either apoptosis or cellular senescence. Thus, maintaining telomere length is essential for cell survival. Telomerase is the enzyme that maintains telomere length. During normal DNA replication, telomeres shorten due to the inability of the replication machinery to fully copy the very ends of chromosomes. The natural shortening is counterbalanced by telomerase, which adds telomeric DNA sequence onto chromosome ends (28). Telomerase has two conserved core subunits: an essential RNA component, TR, and a catalytic protein component, TERT, as well as a number of species-specific accessory factors (8). Telomerase establishes a length equilibrium that is tightly regulated in the cell by telomere binding proteins and regulatory kinases that regulate the action of telomerase at the telomere (67). Mutations in the telomerase components *TR* and *TERT* that reduce telomerase activity result in telomere shortening in both humans and mice (4, 9, 45, 72, 79). The autosomal dominant inheritance of dyskeratosis congenita, aplastic anemia, and pulmonary fibrosis in individuals carrying telomerase mutations is due to haploinsufficiency when telomerase components are compromised and short telomeres result (4, 5, 49, 70, 72, 79).

We generated and characterized a telomerase-null mouse to understand the connection between telomere length and telomerase (9). The RNA component, *mTR*, was deleted in this mouse, and initial studies were done on two different genetic backgrounds, the 129/C57BL/6J mixed genetic background (42) and later the C57BL/6J background (33). Both of these laboratory strains of mice have unusually long heterogeneous telomeres compared to those of humans and wild mice (31). When these *mTR*$^{-/-}$ mice were successively interbred for six generations, telomeres shortened with each generation (9). On

* Corresponding author. Mailing address: Department of Molecular Biology and Genetics, The Johns Hopkins University School of Medicine, 603 PCTB, 725 N. Wolfe Street, Baltimore, MD 21205. Phone: (410) 614-6506. Fax: (410) 955-0831. E-mail: cgreider@jhmi.edu.
† These authors contributed equally to this work.
▽ Published ahead of print on 4 April 2011.
‡ The authors have paid a fee to allow immediate free access to this article.

this long-telomere genetic background, no phenotypes were seen for the first three generations. After telomeres were sufficiently short, the late-generation $mTR^{-/-}$ G4 through $mTR^{-/-}$ G6 mice showed a progressive functional decline in tissues with high turnover rates (42). There was a pronounced decrease in testis size due to germ cell apoptosis (32), and significant degenerative effects were also seen in the hematopoietic system, gastrointestinal (GI) tract, and skin (26, 34, 35, 42, 64, 76).

To more fully examine phenotypes associated with short telomeres, we generated $mTR^{+/-}$ and $mTR^{-/-}$ mice on the CAST/EiJ genetic background, which has telomere lengths similar to those of humans (31). While the C57BL/6J $mTR^{-/-}$ mice were instrumental in understanding the role of short telomeres in limiting tumor growth (19, 50), the very heterogeneous and unusually long telomeres on this genetic background make phenotypic analysis difficult. In contrast to C57BL/6J $mTR^{-/-}$ mice, CAST/EiJ $mTR^{-/-}$ mice showed significant defects in tissue renewal in the first generation (29). Further, progressive breeding of CAST/EiJ $mTR^{+/-}$ mice showed haploinsufficiency for telomerase similar to that seen in human autosomal dominant dyskeratosis congenita families. The phenotypes of these mice recapitulate many of the disease phenotypes seen in human dyskeratosis congenita that contribute to the morbidity and mortality of the disease, including bone marrow failure (3, 29). The progressive telomere shortening and decreased survival with each generation in these mice are similar to the genetic anticipation found in dyskeratosis congenita. In these autosomal dominant families, the genetic anticipation describes a worsening of the phenotype and an earlier onset of disease in the later generations (4, 73).

Autosomal dominant dyskeratosis congenita was first found to be caused by loss-of-function mutations in the *hTR* gene (72), and other families were later identified that have mutations in *hTERT* (4). Mutations in either *hTR* or *hTERT* also cause autosomal dominant pulmonary fibrosis (5, 70), indicating that mutation in either *hTR* or *hTERT* can result in haploinsufficiency and telomere shortening (2). Mouse models of *mTR* and *mTERT* deficiency can offer insight into the role of these two components in human disease. The first experiments to look at loss of telomerase function in mammals were done using the *mTR* null allele, as described above. Subsequently, three different groups generated $mTERT^{-/-}$ mice (15, 45, 81). All of these mice were analyzed on C57BL/6J and 129/C57BL/6J mixed genetic backgrounds with long telomeres. Progressive telomere shortening was seen in the embryonic stem cells grown in culture (44, 45) and in successive generations of $mTERT^{-/-}$ mice (22). Similar to the $mTR^{-/-}$ mice, there was no phenotype seen in the early generations (22, 81), while later generations showed degenerative phenotypes in the testes, intestine, and bone marrow (14, 54) similar to those of $mTR^{-/-}$ mice.

To understand the human diseases associated with telomerase, it is important to know whether mutations in *hTR* and *hTERT* would be expected to show similar or different phenotypes. Telomerase mutations in families are typically initially diagnosed as either dyskeratosis congenita or pulmonary fibrosis. However, the clinical manifestations of short telomeres are very heterogeneous. The factors that determine which clinical manifestation may be seen first are not yet clear. Several investigators have suggested that the specific gene that is mutated, *hTR* or *hTERT*, or the specific mutation may play a role in determining which disease is seen (12, 23, 74, 77). Another explanation that has been suggested for the difference in the disease spectrum comes from recent literature suggesting that the TERT protein may have functional roles independent of its role in telomere elongation (16, 24, 47, 51, 60). If, indeed, TERT has additional functions that are separate from telomere length maintenance, it would be expected that some mutations in *hTERT* might be manifested as diseases different than those seen with mutations in *hTR*.

To fully understand the potential spectrum of diseases that are due to mutations in either *hTERT* or *hTR*, we wanted to critically examine the effects of *mTERT* loss and *mTERT* haploinsufficiency in mice. To do this, we took advantage of the CAST/EiJ mouse with short, homogeneous telomere length distributions (31). By examining CAST/EiJ $mTERT^{-/-}$ and $mTERT^{+/-}$ mice and comparing them to CAST/EiJ $mTR^{-/-}$ and $mTR^{+/-}$ mice, we can further determine whether any additional phenotypes are seen that may be attributable to alternative functions of TERT. In our analysis, we found that the telomere shortening in $mTERT^{-/-}$ and $mTERT^{+/-}$ mice was very similar to that observed in $mTR^{-/-}$ and $mTR^{+/-}$ mice. We documented haploinsufficiency in progressive generations of $mTERT^{+/-}$ and $mTERT^{-/-}$ mice that led to a loss of tissue renewal capacity. Moreover, we did not find any additional phenotypes, including Wnt pathway defects, in $mTERT^{-/-}$ mice, suggesting that the phenotypic consequence of *mTERT* loss is caused by telomere shortening, not by telomere-independent functions of mTERT.

MATERIALS AND METHODS

Mouse breeding. *mTERT* CAST/EiJ mice were generated by following the protocol for *mTR* CAST/EiJ mice (29). Briefly, we backcrossed C57BL/6J *mTERT* heterozygous mice (45) onto the CAST/EiJ background for six generations. After six backcrosses, heterozygous mice were designated HG1 for heterozygous generation 1. The progeny of HG1 crosses generated KO_{G2}, HG2, and WT2* mice (see Fig. 1A). Subsequent generations were obtained by interbreeding increasingly heterozygous generations. HG1 mice were maintained by crossing them to wild-type (WT) mice to avoid haploinsufficiency causing telomere shortening. All animals were housed and bred in a pathogen-free environment at The Johns Hopkins University. All procedures were approved by the Institutional Animal Care and Use Committee at The Johns Hopkins University.

Telomere length analysis. We measured telomere length by quantitative fluorescence *in situ* hybridization (Q-FISH) and flow cytometry FISH (Flow-FISH). For Q-FISH, we generated metaphases from splenocytes as described previously (33). Metaphase slides were hybridized with a Cy3-labeled PNA telomere probe (Applied Biosystems) and imaged with a Zeiss Axioskop microscope, and telomere length analysis was performed in a blinded fashion using the TFL-TELO software (63). Flow-FISH was performed on splenocytes by following the protocol of Baerlocher et al. (6). Briefly, we isolated spleens and generated single-cell suspensions using a 70-μm cell strainer (BD Falcon). We removed erythrocytes by lysing them in RBC Lysis Buffer (eBioscience). The remaining white blood cells were washed with phosphate-buffered saline (PBS) and resuspended in hybridization mix (70% formamide [Fisher Scientific], 0.5% blocking reagent [Roche], 0.01 M Tris, 0.4 mg/ml fluorescein isothiocyanate [FITC]-labeled PNA probe [Applied Biosystems]) and incubated at 87°C for 15 min and then overnight at room temperature, both times in the dark. Cells were washed twice on the following day (1% bovine serum albumin [BSA; Roche], 0.01 M Tris, 70% formamide, 0.1% Tween 20 [Sigma]) and resuspended in 0.1% BSA. DNA was stained with 7-aminoactinomycin D (4 μg/ml; Invitrogen) and RNase A treated (0.2 mg/ml; Roche) for 30 min at room temperature in the dark. Samples were run on a FACScalibur flow cytometer (BD Biosciences), and data were analyzed using the FlowJo software. To ensure that the FL-1 channel was within the linear

range of detection and sensitivity, we used FITC-labeled calibration beads (Bangs Laboratories) prior to every run.

Pathology. Mice were euthanized, and organs were fixed in 10% formalin. Where organ architecture needed to be preserved (GI tract, lungs), organs were injected with 10% formalin. Following fixation, organs were embedded in paraffin, sectioned, and stained with hematoxylin and eosin (H&E). For testis analysis, testes were fixed in Bouin's fixative overnight and similarly processed. Testis slides were imaged on a Nikon Eclipse 50i microscope and analyzed using the NIS-Elements imaging software (Nikon). Both pathologic and testis analyses were performed in a blinded fashion. Complete blood counts were done on blood obtained by cardiac puncture of anesthetized mice using heparin-rinsed syringes, placed into EDTA-coated tubes (BD), and sent to the Johns Hopkins medical lab for complete and differential blood counts on the same day. To analyze mouse ribs, mice were sacrificed by CO_2 asphyxiation prior to X-ray analysis and imaged using a Faxitron model MX-20 X-ray machine. To look for subtle Wnt-related phenotypes, embryos from $mTERT^{+/-}$ crosses were dissected at embryonic day 13.5 (E13.5) to E14.5. The gross morphology, including body axis formation, was examined in a blinded manner after dissection. Samples were taken for genotype analysis, and embryos were then fixed in formalin. The lungs and kidneys were dissected and examined for morphological changes. Embryonic heads were processed for paraffin embedding according to standard methods. Ten-micrometer serial coronal sections of the head were cut. Sections 250 μm apart were stained with H&E. The major structures of the brain, including the forebrain, midbrain, and cerebellum, of WT and $mTERT^{-/-}$ mice were compared in a blinded manner by two independent researchers.

Luciferase assay. CAST/EiJ *mTERT* WT2* and KO_{G2} and C57BL/6J WT and *mTERT* knockout (KO) G1 mouse embryonic fibroblasts (MEFs) were split into 24-well plates at a density of 10^4 cells per well and transfected with 200 ng total DNA for 48 h using Fugene-6 (Roche). Transfected DNA contained several plasmids, including 50 ng TOPflash firefly luciferase plasmid, 50 ng Wnt3a plasmid, and 0.8 ng *Renilla* luciferase pTK-RL as a transfection control, and 99.2 ng of DNA for enhanced green fluorescent protein (EGFP). In samples where one or more components were omitted, total DNA was adjusted to 200 ng/well with DNA for EGFP. All plasmids were kindly provided by Jeremy Nathans. After transfection, cells were washed with PBS and luciferase levels were measured using the Dual-Luciferase Reporter Assay System (Promega). Luciferase levels were calculated by dividing firefly luciferase by *Renilla* luciferase levels. Assays were performed at least in triplicate.

Statistical analysis. Statistical significance was calculated with the Prism software (GraphPad) using an unpaired Student *t* test. We considered a *P* value below 0.05 to be statistically significant.

RESULTS

To examine the phenotypes associated with both complete loss of *mTERT* and haploinsufficiency, we crossed the *mTERT* null allele from the C57BL/6J strain (45) onto the CAST/EiJ genetic background by crossing $mTERT^{+/-}$ mice to CAST/EiJ WT mice for six generations. To examine the effects of progressive telomere shortening, we then intercrossed the heterozygous mice for nine generations (Fig. 1A). We designated each successive heterozygous generation HG1 through HG9 as previously described for $mTR^{+/-}$ mice (29). The $mTERT^{-/-}$ "knockouts" from each generation were designated KO_{G2} through KO_{G9}, and the WT littermates were designated WT2* through WT9* (3). $mTERT^{+/-}$ mice on the C57BL/6J background were previously shown to have 50% of the *mTERT* transcript level of WT mice (45). We confirmed a similar decrease in *mTERT* mRNA in the bone marrow, liver, and MEFs of the CAST/EiJ mouse strain by using quantitative reverse transcription-PCR (data not shown).

Telomere shortening in $mTERT^{-/-}$ and $mTERT^{+/-}$ mice is similar to shortening in $mTR^{-/-}$ and $mTR^{+/-}$ mice. We first examined the telomere lengths in WT, $mTERT^{+/-}$, and $mTERT^{-/-}$ mice by Q-FISH (63). There was significant telomere shortening in $mTERT^{-/-}$ mice compared to WT mice (Fig. 1B), and two heterozygous littermates from this cross were intermediate in telomere length (Fig. 1C). This shows that haploinsufficiency for *mTERT* leads to shorter telomeres in one generation. To compare telomere shortening in $mTERT^{-/-}$ mice to the shortening that occurs in $mTR^{-/-}$ mice, we used Q-FISH on splenocyte metaphases prepared from generation- and age-matched mice. The degree of telomere shortening of $mTERT^{-/-}$ mice (Fig. 1D) was indistinguishable from that of $mTR^{-/-}$ mice (Fig. 1E). This indicates that loss of telomerase activity, whether from loss of *mTR* or loss of *mTERT*, leads to a very similar degree of telomere shortening.

To examine individual mice in successive generations of heterozygous breeding, we used the Flow-FISH protocol (6). Using this method, we first examined littermates from a cross of $mTERT^{+/-}$ HG5 mice and compared the telomere lengths to those of WT mice from our CAST/EiJ colony (Fig. 2A). The *mTERT* KO_{G6} mice had the shortest telomeres, followed by the $mTERT^{+/-}$ HG6 and WT6* mice. The $mTERT^{+/+}$ WT6* mice show inheritance of short telomeres, as was seen for the WT* mice from late-generation heterozygous crosses of $mTR^{+/-}$ mice (3, 29).

To examine whether there is progressive telomere shortening with successive generations in $mTERT^{+/-}$ mice, we compared the telomere length in two HG1 mice to that in two HG7 mice. The later-generation $mTERT^{+/-}$ HG7 mice had considerably shorter telomeres, indicating that *mTERT* is haploinsufficient (Fig. 2B). We also saw mouse-to-mouse variation in telomere length that was particularly evident in two HG7 littermates. This mouse-to-mouse variation has been noted previously in Q-FISH experiments (Fig. 1D and B) (unpublished data) and was confirmed by the analysis of six unrelated, age-matched WT mice (Fig. 2C and D). This mouse-to-mouse variation is likely due to the random inheritance of different numbers of long and short telomeres from the parents (2). Telomere length on any given chromosome end varies independently of the chromosome identity, and random segregation at meiosis then allows such individual variation to occur within litters (33).

Decreased survival with progressive breeding of $mTERT^{+/-}$ mice. To examine the phenotypes that are due to the loss or haploinsufficiency of *mTERT*, we examined the survival of $mTERT^{-/-}$ KO_{G2} and KO_{G3} mice derived from progressive generations of $mTERT^{+/-}$ mice. The survival of $mTERT^{-/-}$ mice decreased with progressive generations of breeding. The median survival of the WT mice in our colony was 627 days ($n = 45$). This survival decreased in KO_{G2} mice born to HG1 parents (median, 452 days; $n = 82$) and further decreased in KO_{G3} mice born to HG2 parents (median, 372 days; $n = 36$) (Fig. 3A). Coincident with the decreased survival, there was also a decrease in body weight in the $mTERT^{-/-}$ mice with short telomeres (Fig. 3B). This decreased body weight is similar to that in $mTR^{+/-}$ mice and may be due to bone marrow failure, malabsorption secondary to the gastrointestinal defects, or typhlocolitis, an inflammation of the colon secondary to bone marrow failure (2).

$mTERT^{+/-}$ and $mTERT^{-/-}$ mice show phenotypes associated with human syndromes of telomere shortening. To establish the underlying cause of the decreased survival time in the $mTERT^{+/-}$ breeding colony, we carried out complete necropsy of WT, $mTERT^{+/-}$, and $mTERT^{-/-}$ mice under a protocol in

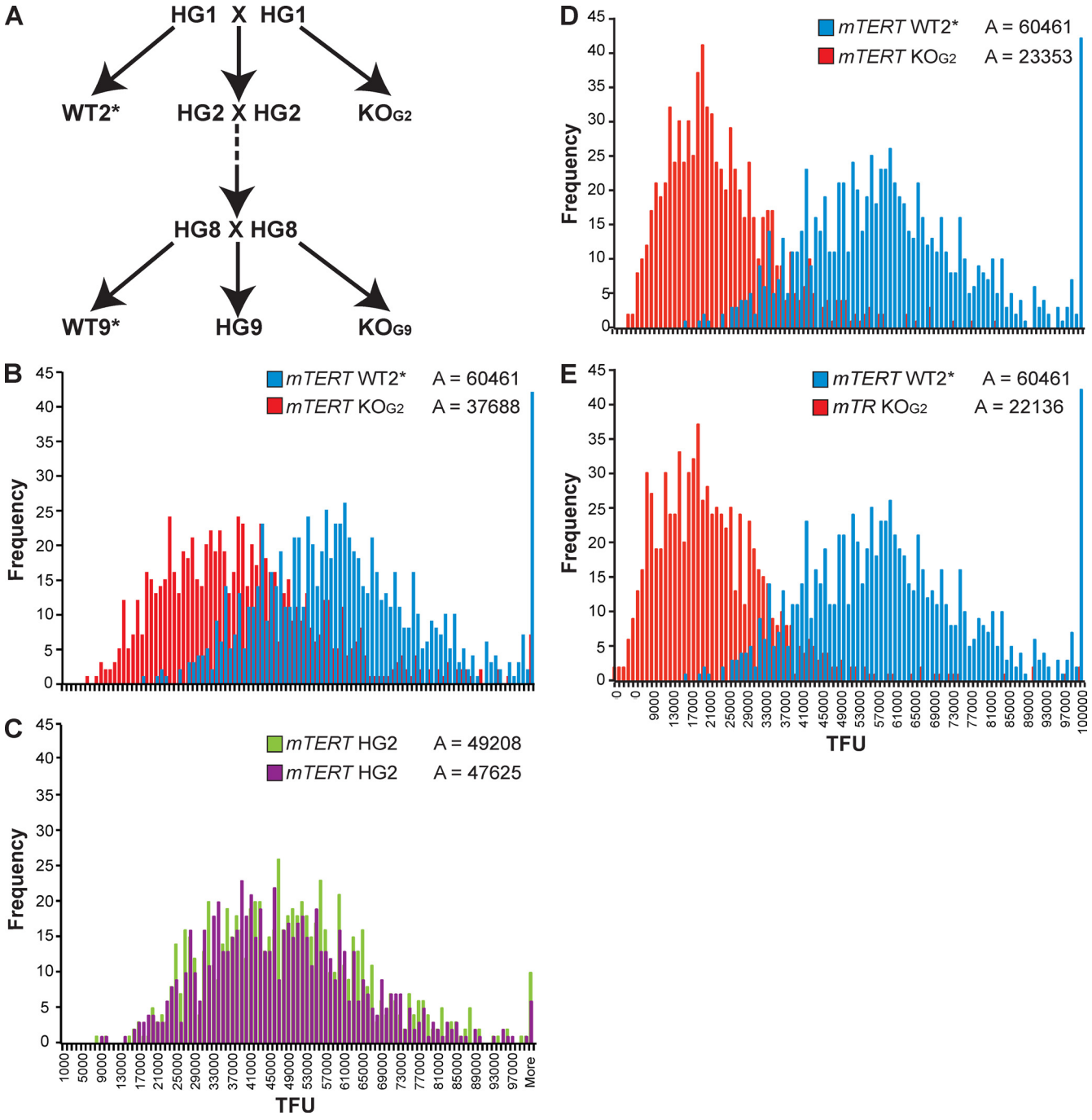

FIG. 1. *mTERT*$^{-/-}$ and *mTERT*$^{+/-}$ mice show telomere shortening and haploinsufficiency. (A) CAST/EiJ *mTERT*$^{+/-}$ breeding scheme and nomenclature of each generation. (B and C) Q-FISH analysis of littermates from an *mTERT*$^{+/-}$ HG1 cross. TFU represents arbitrary telomere fluorescence units. *mTERT*$^{-/-}$ KO_{G2} (mean = 37,688 TFU) and WT WT2* (mean = 60,461 TFU) (B) and two *mTERT*$^{+/-}$ HG2 littermates (C) are compared on the same scale (means = 49,208 and 47,625 TFU, respectively). (D) Telomere length distribution in *mTERT* KO_{G2} (mean = 23,353 TFU) and (E) *mTR* KO_{G2} mice (mean = 22,136 TFU) compared to that in WT mice (mean = 60,461 TFU).

which the pathologist did not know the genotype of the mice under study. The *mTERT*$^{-/-}$ mice showed the most severe phenotypes, including intestinal villous atrophy and crypt depletion, occasional crypt hyperplasia and microadenomas, typhlocolitis in the large intestine, atrophy of the seminiferous tubules, extramedullary hematopoiesis (EMH) in the liver and spleen, and a skewed myeloid/erythroid ratio in the bone marrow. Consistent with the haploinsufficiency seen in telomere length maintenance, *mTERT*$^{+/-}$ mice also showed similar pathology, although it was less severe than in the null animals, including a skewed myeloid/erythroid ratio, EMH, and intestinal atrophy.

To more carefully examine the phenotypes seen in pathology, we quantitated the appearance of abnormal seminiferous

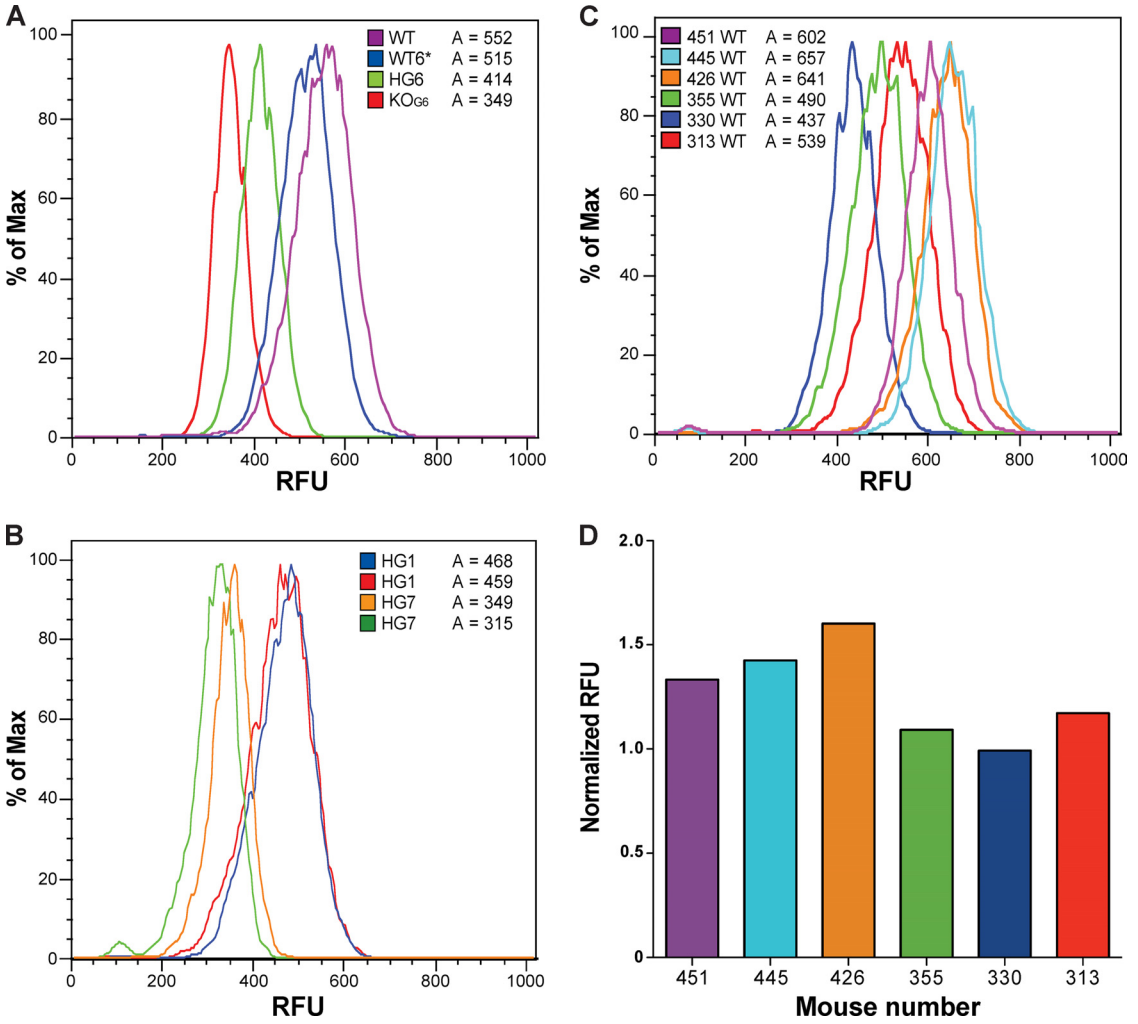

FIG. 2. Telomere length decreases in *mTERT*$^{-/-}$ and *mTERT*$^{+/-}$ mice analyzed by Flow-FISH. (A) Flow-FISH analysis of telomere length within one litter and compared to that in WT mice. RFU is relative fluorescence units of the telomere signal (means: WT = 552 RFU, WT6* = 515 RFU, HG6 = 414 RFU, and KO_{G6} = 349 RFU). (B) Telomere length comparison of two HG1 mice to two HG7 mice by Flow-FISH (geometric means: HG1 = 468 RFU, HG1 = 459 RFU, HG7 = 349 RFU, and HG7 = 315 RFU). (C) Flow-FISH analysis of six independent WT mice shows heterogeneity within mice of the same genotype. The numbers indicate the numbers of mice in our colony. (D) The quantitative Flow-FISH value, normalized RFU to bovine thymocytes as an internal control, is shown for each mouse analyzed in panel C.

tubules in the testes. Telomere shortening in germ cells leads to apoptosis in the testes (32, 42), which is evident in H&E-stained sections as hypocellular seminiferous tubules. We compared age-matched WT, *mTERT*$^{+/-}$, and *mTERT*$^{-/-}$ mice and found a significant increase in hypocellular tubules in both *mTERT*$^{+/-}$ and *mTERT*$^{-/-}$ mice, although the phenotype was most pronounced in *mTERT*$^{-/-}$ mice, where telomeres were significantly shorter (Fig. 4A and B).

Loss of tissue renewal due to short telomeres is seen in several proliferative organs. The whole animal pathology indicated there was significant villous atrophy in the small intestine (Fig. 4C) and large intestine (Fig. 4E) in *mTERT*$^{-/-}$ mice. We quantitated the degree of atrophy in H&E-stained sections from *mTERT*$^{-/-}$ mice (Fig. 4D). *mTERT*$^{-/-}$ mice showed both significant villous atrophy and microadenomas in regions adjacent to regions of atrophy (Fig. 4C). This appearance of microadenomas is similar to what was found in *mTR*$^{-/-}$ mice and indicates that short telomeres, in addition to loss of tissue renewal, may sometimes lead to neoplastic growth (3, 29). The defect in the *mTERT*$^{+/-}$ mice was more subtle and was seen only in one older mouse. This lower penetrance of the intestinal villous atrophy in *mTERT*$^{+/-}$ mice than in *mTR*$^{+/-}$ mice is likely due to the fact that the *mTR*$^{+/-}$ colony was established 7 years earlier and has undergone additional telomere shortening during breeding, allowing phenotypes due to haploinsufficiency to be manifested.

Aplastic anemia is a common manifestation of telomere shortening in human patients with dyskeratosis congenita (7, 40). The EMH seen in the mouse is indicative of bone marrow failure. To examine potential bone marrow dysfunction, we performed complete blood cell counts and found a significant decrease in the total white blood cell counts of *mTERT*$^{+/-}$ (P = 0.0007) and *mTERT*$^{-/-}$ mice (P = 0.0007) (Fig. 4F). These decreased white blood cell counts are indicative of bone marrow dysfunction in mice with short telomeres. Therefore, the spectrum of pathological changes seen in *mTERT*$^{+/-}$ mice

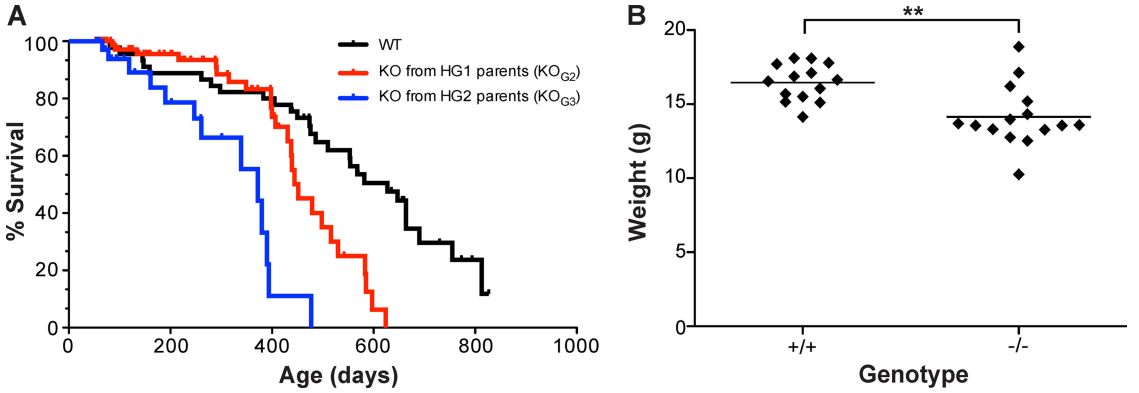

FIG. 3. *mTERT*$^{-/-}$ mice have decreased survival and body weights. (A) Kaplan-Meier survival curve for WT (n = 45), KO$_{G2}$ (n = 82), and KO$_{G3}$ (n = 36) mice (median survival: WT = 627 days; KO$_{G2}$ = 452 days; KO$_{G3}$ = 372 days). (B) Body weight analysis of WT (n = 14, average weight = 16.47 g) and *mTERT*$^{-/-}$ (KO$_{G2}$ through KO$_{G6}$, n = 15; average weight = 14.15 g) mice. ** indicates P = 0.0011.

is similar to that previously characterized in *mTR*$^{+/-}$ mice and in dyskeratosis congenita patients.

***mTERT*$^{-/-}$ mice show no additional phenotypes not seen in *mTR*$^{-/-}$ mice.** Recent experiments have suggested that TERT may have additional roles in cell growth independent of its function at telomeres (17, 55). Mice overexpressing *mTERT* show excessive hair growth (65). In contrast, we examined but did not find hair loss in *mTERT*$^{-/-}$ mice, indicating that ab-

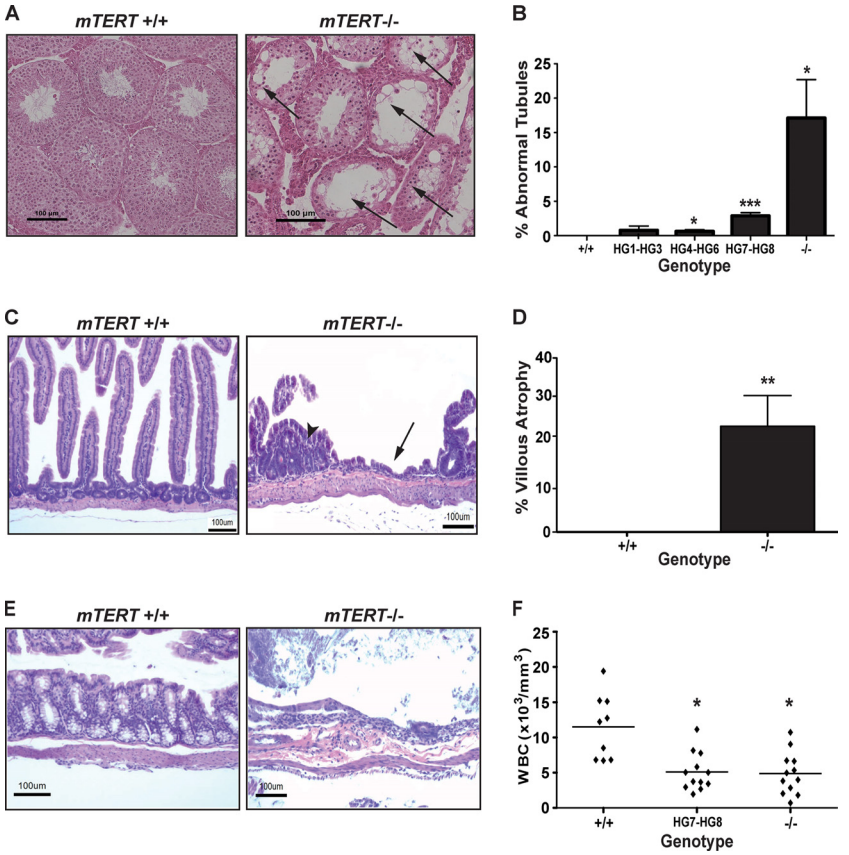

FIG. 4. *mTERT*$^{-/-}$ and *mTERT* $^{+/-}$ mice show defects in tissue renewal. (A) H&E staining of testis sections from WT (left panel) and *mTERT*$^{-/-}$ mice (right panel). Arrows show abnormal or empty tubules (magnification, ×100; scale bar = 100 μm). (B) Quantitation of abnormal tubules in *mTERT*$^{+/-}$ (HG1-HG3, n = 5; HG4-HG6, n = 6; HG7-HG8, n = 12) and *mTERT*$^{-/-}$ (n = 7) mice compared to those of WT (+/+, n = 7) mice. * indicates $P < 0.05$; *** indicates P = 0.0002. (C) H&E staining of small intestine sections from WT (left panel) and *mTERT*$^{-/-}$ (right panel) mice. Arrow indicates area of villous atrophy, and arrowhead indicates microadenoma (magnification, ×100; scale bar = 100 μm). (D) Quantitation of percent villous atrophy in the GI tracts of WT (+/+, n = 5) and *mTERT*$^{-/-}$ (−/−, n = 5) mice. ** indicates P = 0.003. (E) H&E staining of large intestine sections from WT (left panel) and *mTERT*$^{-/-}$ (right panel) mice. (F) White blood cell (WBC) counts of blood from WT (+/+, n = 9), *mTERT*$^{+/-}$ (HG7 and HG8, n = 12), and *mTERT*$^{-/-}$ (n = 12) mice. ** indicates P = 0.0007.

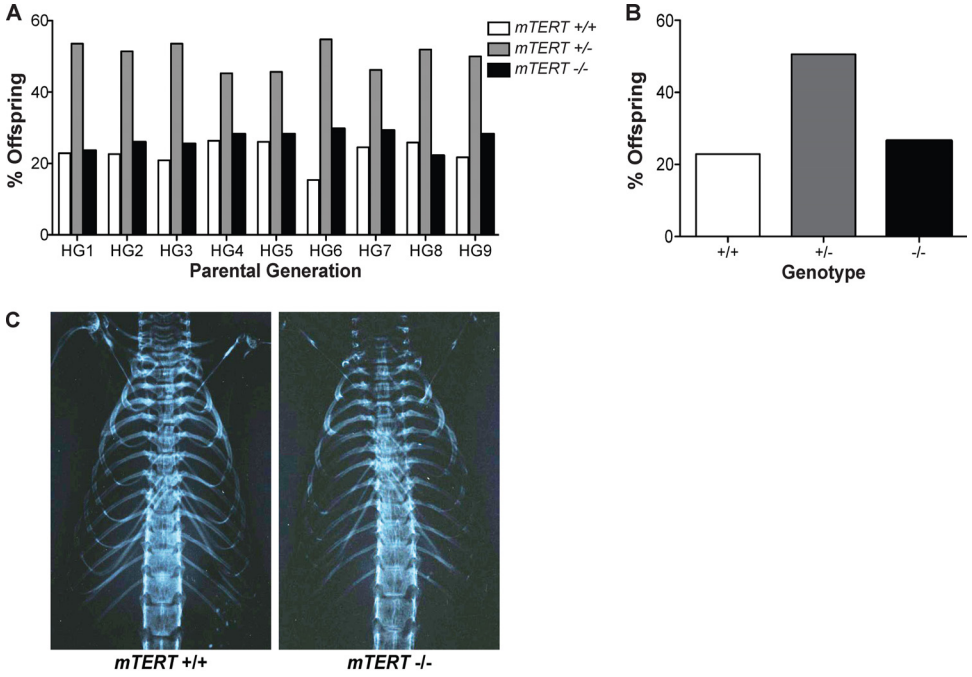

D

	Fraction of mice with normal rib number	
	mTERT+/+	*mTERT*-/-
CAST/EiJ	5/5	15/15
C57BL/6J	12/12	20/20

FIG. 5. $mTERT^{-/-}$ mice are born in expected ratios and show no phenotypes ascribed to Wnt signaling deficiency. (A) Quantitation of Mendelian ratios of progeny from each generation of heterozygous mice. (B) Total genotype distribution from all heterozygous crosses (n = 1,089) from CAST/EiJ $mTERT^{+/-}$ intercrosses: 22.9% WT, 50.6% $mTERT^{+/-}$, and 26.5% $mTERT^{-/-}$. (C) X rays to examine rib numbers in CAST/EiJ $mTERT^{+/+}$ and $mTERT^{-/-}$ mice. (D) Quantitation of rib numbers from X rays of WT and $mTERT^{-/-}$ mice in both the CAST/EiJ and C57BL/6J genetic backgrounds.

sence of TERT does not affect hair growth. The TERT protein has also been suggested to play a role in the Wnt signaling pathway independent of its role at telomeres (16, 60). Most Wnt pathway mutant mice ($Wnt1^{-/-}$ through $Wnt\ 11^{-/-}$) have severe developmental defects and die embryonically or right after birth (46). To determine whether we might have missed a class of mice that die embryonically due to Wnt pathway defects, we first examined the ratios of genotypes of adult offspring from our crosses. Crosses of heterozygous CAST/EiJ $mTERT^{+/-}$ mice yielded expected Mendelian ratios of 23% +/+, 51% +/−, and 26% −/− mice, with 1,089 mice examined (Fig. 5A and B). Thus, we find no evidence of loss of the $mTERT^{-/-}$ genotype due to embryonic defects.

To examine possible Wnt pathway phenotypes, we examined organs of adult $mTERT^{-/-}$ mice. Blinded examination of H&E-stained sections revealed no defects in the lungs, kidneys, heart, or urogenital tract in $mTERT^{-/-}$ mice. A previous publication (60) suggested that some $mTERT^{-/-}$ mice have missing ribs, which was interpreted as a Wnt pathway developmental defect. To look specifically at rib numbers, we examined X rays of both WT and $mTERT^{-/-}$ CAST/EiJ mice (n = 15), as well as WT and $mTERT^{-/-}$ C57BL/6J mice (n = 20) (Fig. 5C). All of the mice examined showed the normal number and appearance of ribs (Fig. 5D).

While most Wnt KO mice have severe developmental defects, it has been suggested that severe Wnt pathway defects may not be seen in adult $mTERT^{-/-}$ mice due to developmental compensation (60). To determine whether there may be subtle defects in the Wnt pathway in early development that may be compensated for to allow survival, we examined embryos from crosses of CAST/EiJ $mTERT^{+/-}$ mice. To guide our analysis, we examined specific phenotypes seen in Wnt gene KO mice. $Wnt4^{-/-}$, $Wnt9b^{-/-}$, and $Wnt11^{-/-}$ mice show defects in kidney development (38, 48, 68). $Wnt2/2b^{-/-}$ mice show defects in lung development (25, 59). Defects in axis development, including a truncated axis and truncated limbs, are seen in $Wnt3^{-/-}$, $Wnt5a^{-/-}$, and $Wnt7a^{-/-}$ mice (43, 61, 80). Runting and small embryo size are found in several mutants, including $Wnt2^{-/-}$ mice (59). Urogenital defects are seen in $Wnt7^{-/-}$ and $Wnt\ 9b^{-/-}$ mice (13, 56). Finally, failure of the midbrain and cerebellum to develop is found in $Wnt1^{-/-}$ mice (52, 53, 69). To determine whether these phenotypes are seen in $mTERT^{-/-}$ mice, we dissected 58 embryos from $mTERT^{+/-}$ intercrosses. WT and $mTERT^{-/-}$ embryos were examined in a blinded fashion by two experts familiar with Wnt developmental defects. The $mTERT^{-/-}$ embryos showed no gross morphological differences; we did not find evidence of axis truncation, limb truncation, or smaller embryo size (Fig. 6A and B). Embryos were dissected, and the lungs and kidneys were examined for morphological defects (Fig. 6C and D). We

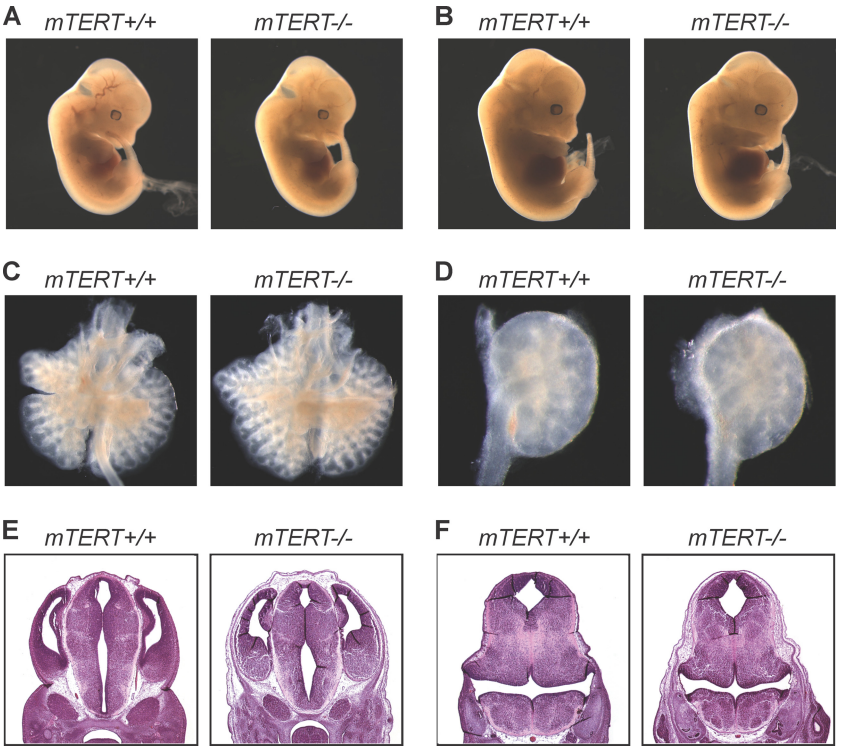

FIG. 6. $mTERT^{-/-}$ embryos show no phenotypes ascribed to Wnt signaling deficiency. To look for subtle phenotypes, 58 embryos were dissected and evaluated in a blinded fashion. Representative examples are shown. E13.5 (A) and E14.5 (B) WT (left panels) and $mTERT^{-/-}$ (right panels) whole embryos (magnification, ×0.8; $n = 12$ each) are shown. (C) Embryonic lungs dissected from WT (left panel) and $mTERT^{-/-}$ (right panel) embryos at E14.5 (magnification, ×3.2; $n = 3$ each). (D) Embryonic kidneys dissected from WT (left panel) and $mTERT^{-/-}$ (right panel) embryos at E14.5 (magnification, ×6.6; $n = 3$ each). Also shown are H&E-stained midbrain (E) and cerebellar primordium (F) sections from E14.5 WT (left panels) and $mTERT^{-/-}$ (right panels) embryos (magnification, ×2.5; $n = 3$ each).

also examined embryonic brain sections for defects in the midbrain and cerebellum (Fig. 6E and F). We found no differences between WT and $mTERT^{-/-}$ embryos in any of the tissues examined. Our phenotypic data from Mendelian ratios and adult and embryonic tissues showed no evidence of Wnt pathway defects in two different genetic backgrounds.

To directly investigate whether absence of TERT affects Wnt signaling, we used a functional readout of Wnt-induced transcriptional activity. CAST/EiJ and C57BL/6J WT and $mTERT^{-/-}$ MEFs were transformed with the TOPflash reporter plasmid, which contains 7 tandem TCF binding sites driving the luciferase reporter gene (58). To specifically activate the Wnt pathway, these cells were cotransfected with a plasmid that allows expression of the Wnt3a ligand

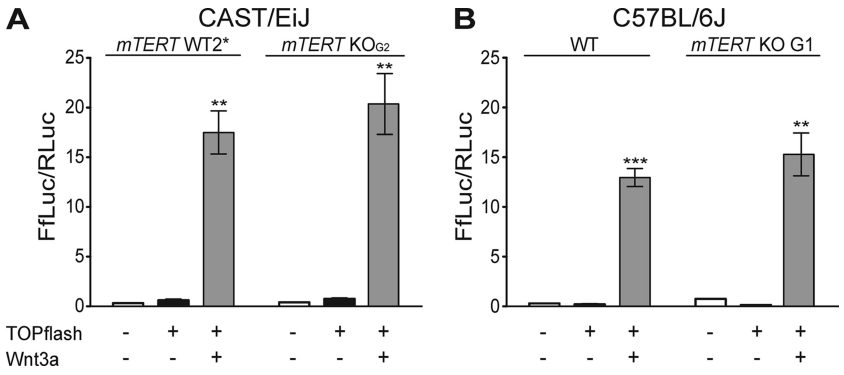

FIG. 7. $mTERT^{-/-}$ cells show Wnt pathway signaling activation similar to that of WT cells *in vitro*. Luciferase activity was measured in MEFs transfected with the TOPflash reporter plasmid and a control *Renilla* luciferase reporter, with and without Wnt3a ligand (see Materials and Methods), as indicated below the graphs. (A) TOPflash luciferase assay of CAST/EiJ *mTERT* WT2* (**, $P = 0.0015$, relative to basal activation) and *mTERT* KO_{G2} (**, $P = 0.0031$, relative to basal activation) MEFs. (B) TOPflash luciferase assay of C57BL/6J WT (***, $P = 0.0021$, relative to basal activation) and *mTERT* KO G1 (**, $P = 0.0001$, relative to basal activation) MEFs.

and luciferase levels were measured. As a control, we measured the uninduced level of luciferase in cells that did not receive the Wnt3a plasmid, as well as in untransfected cells. The levels of luciferase in WT and $mTERT^{-/-}$ cells were indistinguishable ($P = 0.487$) (Fig. 7A). Since previous experiments indicating that TERT overexpression activates the Wnt pathway were done in the C57BL/6J background, we repeated the luciferase reporter experiments with WT and $mTERT^{-/-}$ MEFs from C57BL/6J mice (Fig. 7B) and again saw no difference in luciferase levels between WT and $mTERT^{-/-}$ cells ($P = 0.37$). Thus, we conclude that loss of TERT does not affect the Wnt signaling pathway.

DISCUSSION

Mutations in the telomerase components *hTERT* and *hTR* lead to a spectrum of diseases of telomere shortening, including dyskeratosis congenita, pulmonary fibrosis, aplastic anemia, and liver disease, among others (2, 7, 75). To understand whether these disease phenotypes in humans are likely to all be due to telomere shortening or if some may be due to alternative functions of TERT, we examined the pathology in CAST/EiJ $mTERT^{+/-}$ and $mTERT^{-/-}$ mice in detail. We found that *mTERT* deficiency produces a phenotype indistinguishable from that due to *mTR* deficiency and worsens with each generation, indicating that short telomeres mediate disease in both mutant backgrounds.

Haploinsufficiency for *mTERT* results in telomere shortening and loss of tissue renewal. We found progressive telomere shortening with successive breeding of $mTERT^{+/-}$ mice, indicating that loss of one allele of *mTERT* results in haploinsufficiency. While one previous study suggested that *mTERT* did not show haploinsufficiency (15), three recent studies that examined successive generations of $mTERT^{+/-}$ mice on the C57BL/6J genetic background found progressive telomere shortening (14, 22, 54). However, these studies using C57BL/6J $mTERT^{+/-}$ mice did not find phenotypic changes in later-generation heterozygotes using two different heterozygous breeding schemes (14, 54). In contrast, we found with both CAST/EiJ $mTR^{+/-}$ (3, 29) and $mTERT^{+/-}$ (this report) mice that the progressive telomere shortening with each generation is associated with a progressive decline in organ function, similar to the genetic anticipation seen in dyskeratosis congenita patients. Since many phenotypes in CAST/EiJ $mTR^{+/-}$ and $mTERT^{+/-}$ heterozygous mice are initially subtle in early generations, it is likely that the lack of phenotype expression in C57BL/6J mice is due to insufficient telomere shortening. C57BL/6J mice have unusually long and heterogeneous telomeres, and thus, the consequences of telomere shortening are not seen for many generations, even in the null background (14, 42, 54). CAST/EiJ mice have both more homogeneous and shorter telomere length distributions, similar to humans; thus, the effects of short telomeres are manifested more clearly in these mice.

Loss of *mTERT* does not affect Wnt signaling. The TERT protein has been reported to function in several pathways that are independent of telomere length regulation. Overexpression of *mTERT* has been reported to stimulate hair follicle stem cell proliferation (65), activate transcription of the Wnt and c-myc transcriptional pathways (16, 60, 66), and affect the transforming growth factor beta regulatory pathway (24). In addition, in one study, knockdown of *hTERT* was implicated in the DNA damage response (51). In contrast to these results, two independent studies have examined $mTERT^{-/-}$ cells and found no evidence of a change in the DNA damage response (21, 71). In addition, whole-genome transcriptional analysis of C57BL/6J $mTERT^{-/-}$ G1 MEFs and tissues revealed no genes, including genes in the Wnt and DNA damage pathways, that were specifically up- or downregulated compared to those in WT cells (71). Here we functionally examined Wnt transcriptional pathway activation by using the TOPflash reporter assay and found similar levels of activation in WT and $mTERT^{-/-}$ cells.

How can we reconcile the activation of Wnt pathway genes in *mTERT* overexpression with the lack of changes in Wnt signaling when *mTERT* is deleted? It is possible that high-level overexpression of TERT generates a new gain-of-function phenotype that activates the Wnt pathway. Our studies argue that this effect of TERT is not part of its normal physiological function. Such generation of a neomorph upon high-level overexpression has a precedent in the genetic literature (37, 82). The activation of the Wnt pathway could play a role in some situations when TERT is overexpressed, even though this is not the normal role of TERT in most cells.

$mTERT^{-/-}$ mice show no unexpected phenotypes. While studies of $mTERT^{-/-}$ cells in culture allowed the examination of transcriptional and DNA damage pathways (21, 71), careful analysis of the $mTERT^{-/-}$ mouse can allow phenotypes to be assessed in an unbiased manner. If TERT has essential functions other than telomere lengthening, we would expect to see phenotypes associated with those essential functions in $mTERT^{-/-}$ mice. In one study, $mTERT^{-/-}$ mice were reported to have aberrant numbers of ribs, which is suggestive of a Wnt pathway developmental defect (60). We found that $mTERT^{-/-}$ mice do not die embryonically, as do most *Wnt* mutant mice. Adult mice also did not show characteristic Wnt-related defects in the lungs, kidneys, or urogenital tract, and there was no evidence of a rib number defect. Previous reports of rib number variation may be due to mouse strain phenotypic variability, as has been previously reported (10, 27, 39). Examination of $mTERT^{-/-}$ embryos and embryonic tissues also revealed no subtle Wnt phenotypes. Finally, while TERT function has recently been linked to mitochondrial RNA processing endoribonuclease (RMRP) (47), the blinded total necropsy we performed showed no overt phenotypes in $mTERT^{-/-}$ mice that might be expected from RMRP deficiency. The phenotypes that we did find in $mTERT^{-/-}$ mice are very similar to those seen in $mTR^{-/-}$ mice, consistent with the notion that short telomeres mediate these effects.

***mTR* and *mTERT* produce indistinguishable phenotypes: implications for human disease.** The phenotypes seen in $mTERT^{+/-}$ and $mTR^{+/-}$ mice were remarkably similar to each other and recapitulate the phenotypes seen in human disease. In humans, mutations in both *hTR* and *hTERT* lead to autosomal dominant disease. Our evidence of haploinsufficiency and progressive disease onset in both $mTERT^{+/-}$ and $mTR^{+/-}$ mice is consistent with the genetic anticipation found in these families. It is still not known why some families with telomerase mutations present with dyskeratosis congenita and others present first with pulmonary fibrosis. Because of disease het-

erogeneity, it has been suggested that perhaps the disease spectrum may differ, depending on whether there are mutations in *hTR* or *hTERT* (23, 74, 77). Our analysis of the null phenotype for loss of either TERT or TR indicates that, in an isogenic genetic background, the phenotypes of mutations in these two components are indistinguishable. Recent studies indicate that a single mutant allele can cause heterogeneous phenotypes within a family where pulmonary fibrosis is seen in earlier generations and aplastic anemia becomes the predominant phenotype in later generations (62). This evidence further indicates that it is not the specific mutations in either *hTERT* or *hTR* that determine the disease spectrum, but rather telomere length.

In summary, we have found that loss of the protein component of telomerase, TERT, and loss of the RNA component, TR, result in indistinguishable phenotypes, suggesting that all of the phenotypes we observed are due to telomere shortening. We find no evidence of a phenotypic expression of proposed alternative functions of TERT. Understanding all of the potential manifestations of *hTERT* and *hTR* mutations has important implications for human disease. Our findings make it unlikely that specific diseases will be specifically associated with mutations in the two different components. Effort can therefore be focused on understanding how telomere shortening influences disease expression in different tissues. The ability to study the phenotype in heterozygous mice that mimic the genetic anticipation and haploinsufficiency in humans makes this a powerful model for understanding the consequences of telomere shortening.

ACKNOWLEDGMENTS

We thank Mary Armanios, Brendan Cormack, and Jeremy Nathans for critical reading of the manuscript and Jeremy Nathans for advice and assistance in evaluating embryos for Wnt phenotypes, as well as kindly providing the luciferase assay vectors. We thank the anonymous reviewers, whose comments on the manuscript helped us to strengthen and focus our findings.

This work was supported by a grant from the National Institutes of Health, RO1AG027406.

REFERENCES

1. **Alder, J. K., et al.** 2008. Short telomeres are a risk factor for idiopathic pulmonary fibrosis. Proc. Natl. Acad. Sci. U. S. A. **105:**13051–13056.
2. **Armanios, M.** 2009. Syndromes of telomere shortening. Annu. Rev. Genomics Hum. Genet. **10:**45–61.
3. **Armanios, M., et al.** 2009. Short telomeres are sufficient to cause the degenerative defects associated with aging. Am. J. Hum. Genet. **85:**823–832.
4. **Armanios, M., et al.** 2005. Haploinsufficiency of telomerase reverse transcriptase leads to anticipation in autosomal dominant dyskeratosis congenita. Proc. Natl. Acad. Sci. U. S. A. **102:**15960–15964.
5. **Armanios, M. Y., et al.** 2007. Telomerase mutations in families with idiopathic pulmonary fibrosis. N. Engl. J. Med. **356:**1317–1326.
6. **Baerlocher, G. M., I. Vulto, G. de Jong, and P. M. Lansdorp.** 2006. Flow cytometry and FISH to measure the average length of telomeres (flow FISH). Nat. Protoc. **1:**2365–2376.
7. **Bessler, M., D. B. Wilson, and P. J. Mason.** 2010. Dyskeratosis congenita. FEBS Lett. **584:**3831–3838.
8. **Blackburn, E. H., and K. Collins.** 21 July 2010. Telomerase: an RNP enzyme synthesizes DNA. Cold Spring Harb. Perspect. Biol. [Epub ahead of print.] doi:10.1101/cshperspect.a003558.
9. **Blasco, M. A., et al.** 1997. Telomere shortening and tumor formation by mouse cells lacking telomerase RNA. Cell **91:**25–34.
10. **Branch, S., J. M. Rogers, C. F. Brownie, and N. Chernoff.** 1996. Supernumerary lumbar rib: manifestation of basic alteration in embryonic development of ribs. J. Appl. Toxicol. **16:**115–119.
11. **Calado, R. T., et al.** 2009. A spectrum of severe familial liver disorders associate with telomerase mutations. PLoS One **4:**e7926.
12. **Carroll, K. A., and H. Ly.** 2009. Telomere dysfunction in human diseases: the long and short of it! Int. J. Clin. Exp. Pathol. **2:**528–543.
13. **Carroll, T. J., J. S. Park, S. Hayashi, A. Majumdar, and A. P. McMahon.** 2005. Wnt9b plays a central role in the regulation of mesenchymal to epithelial transitions underlying organogenesis of the mammalian urogenital system. Dev. Cell **9:**283–292.
14. **Chiang, Y. J., et al.** 2010. Telomere length is inherited with resetting of the telomere set-point. Proc. Natl. Acad. Sci. U. S. A. **107:**10148–10153.
15. **Chiang, Y. J., et al.** 2004. Expression of telomerase RNA template, but not telomerase reverse transcriptase, is limiting for telomere length maintenance in vivo. Mol. Cell. Biol. **24:**7024–7031.
16. **Choi, J., et al.** 2008. TERT promotes epithelial proliferation through transcriptional control of a Myc- and Wnt-related developmental program. PLoS Genet. **4:**e10.
17. **Cong, Y., and J. W. Shay.** 2008. Actions of human telomerase beyond telomeres. Cell Res. **18:**725–732.
18. **d'Adda di Fagagna, F., et al.** 2003. A DNA damage checkpoint response in telomere-initiated senescence. Nature **426:**194–198.
19. **de Lange, T., and T. Jacks.** 1999. For better or worse? Telomerase inhibition and cancer. Cell **98:**273–275.
20. **Enomoto, S., L. Glowczewski, and J. Berman.** 2002. MEC3, MEC1, and DDC2 are essential components of a telomere checkpoint pathway required for cell cycle arrest during senescence in Saccharomyces cerevisiae. Mol. Biol. Cell **13:**2626–2638.
21. **Erdmann, N., and L. A. Harrington.** 2009. No attenuation of the ATM-dependent DNA damage response in murine telomerase-deficient cells. DNA Repair (Amsterdam) **8:**347–353.
22. **Erdmann, N., Y. Liu, and L. Harrington.** 2004. Distinct dosage requirements for the maintenance of long and short telomeres in mTert heterozygous mice. Proc. Natl. Acad. Sci. U. S. A. **101:**6080–6085.
23. **Garcia, C. K., W. E. Wright, and J. W. Shay.** 2007. Human diseases of telomerase dysfunction: insights into tissue aging. Nucleic Acids Res. **35:**7406–7416.
24. **Geserick, C., A. Tejera, E. Gonzalez-Suarez, P. Klatt, and M. A. Blasco.** 2006. Expression of mTert in primary murine cells links the growth-promoting effects of telomerase to transforming growth factor-beta signaling. Oncogene **25:**4310–4319.
25. **Goss, A. M., et al.** 2009. Wnt2/2b and beta-catenin signaling are necessary and sufficient to specify lung progenitors in the foregut. Dev. Cell **17:**290–298.
26. **Goytisolo, F. A., et al.** 2000. Short telomeres result in organismal hypersensitivity to ionizing radiation in mammals. J. Exp. Med. **192:**1625–1636.
27. **Green, E. L.** 1941. Genetic and non-genetic factors which influence the type of the skeleton in an inbred strain of mice. Genetics **26:**192–222.
28. **Greider, C. W., and E. H. Blackburn.** 1985. Identification of a specific telomere terminal transferase activity in *Tetrahymena* extracts. Cell **43:**405–413.
29. **Hao, L. Y., et al.** 2005. Short telomeres, even in the presence of telomerase, limit tissue renewal capacity. Cell **123:**1121–1131.
30. **Harley, C. B., A. B. Futcher, and C. W. Greider.** 1990. Telomeres shorten during ageing of human fibroblasts. Nature **345:**458–460.
31. **Hemann, M. T., and C. W. Greider.** 2000. Wild-derived inbred mouse strains have short telomeres. Nucleic Acids Res. **28:**4474–4478.
32. **Hemann, M. T., et al.** 2001. Telomere dysfunction triggers developmentally regulated germ cell apoptosis. Mol. Biol. Cell **12:**2023–2030.
33. **Hemann, M. T., M. Strong, L.-Y. Hao, and C. W. Greider.** 2001. The shortest telomere, not average telomere length, is critical for cell viability and chromosome stability. Cell **107:**67–77.
34. **Herrera, E., A. C. Martinez, and M. A. Blasco.** 2000. Impaired germinal center reaction in mice with short telomeres. EMBO J. **19:**472–481.
35. **Herrera, E., et al.** 1999. Disease states associated with telomerase deficiency appear earlier in mice with short telomeres. EMBO J. **18:**2950–2960.
36. **IJpma, A., and C. W. Greider.** 2003. Short telomeres induce a DNA damage response in Saccharomyces cerevisiae. Mol. Biol. Cell **14:**987–1001.
37. **Jacobs, C., and I. Pirson.** 2003. Pitfalls in the use of transfected overexpression systems to study membrane proteins function: the case of TSH receptor and PRA1. Mol. Cell. Endocrinol. **209:**71–75.
38. **Karner, C. M., et al.** 2009. Wnt9b signaling regulates planar cell polarity and kidney tubule morphogenesis. Nat. Genet. **41:**793–799.
39. **Khera, K. S.** 1981. Common fetal aberrations and their teratologic significance: a review. Fundam. Appl. Toxicol. **1:**13–18.
40. **Kirwan, M., and I. Dokal.** 2008. Dyskeratosis congenita: a genetic disorder of many faces. Clin. Genet. **73:**103–112.
41. **Kirwan, M., et al.** 2009. Defining the pathogenic role of telomerase mutations in myelodysplastic syndrome and acute myeloid leukemia. Hum. Mutat. **30:**1567–1573.
42. **Lee, H.-W., et al.** 1998. Essential role of mouse telomerase in highly proliferative organs. Nature **392:**569–574.
43. **Liu, P., et al.** 1999. Requirement for Wnt3 in vertebrate axis formation. Nat. Genet. **22:**361–365.
44. **Liu, Y., H. Kha, M. Ungrin, M. O. Robinson, and L. Harrington.** 2002. Preferential maintenance of critically short telomeres in mammalian cells heterozygous for mTert. Proc. Natl. Acad. Sci. U. S. A. **99:**3597–3602.

45. **Liu, Y., et al.** 2000. The telomerase reverse transcriptase is limiting and necessary for telomerase function in vivo. Curr. Biol. **10:**1459–1462.
46. **Logan, C. Y., and R. Nusse.** 2004. The Wnt signaling pathway in development and disease. Annu. Rev. Cell Dev. Biol. **20:**781–810.
47. **Maida, Y., et al.** 2009. An RNA-dependent RNA polymerase formed by TERT and the RMRP RNA. Nature **461:**230–235.
48. **Majumdar, A., S. Vainio, A. Kispert, J. McMahon, and A. P. McMahon.** 2003. Wnt11 and Ret/Gdnf pathways cooperate in regulating ureteric branching during metanephric kidney development. Development **130:**3175–3185.
49. **Marrone, A., D. Stevens, T. Vulliamy, I. Dokal, and P. J. Mason.** 2004. Heterozygous telomerase RNA mutations found in dyskeratosis congenita and aplastic anemia reduce telomerase activity via haploinsufficiency. Blood **104:**3936–3942.
50. **Maser, R. S., and R. A. DePinho.** 2002. Connecting chromosomes, crisis, and cancer. Science **297:**565–569.
51. **Masutomi, K., et al.** 2005. The telomerase reverse transcriptase regulates chromatin state and DNA damage responses. Proc. Natl. Acad. Sci. U. S. A. **102:**8222–8227.
52. **McMahon, A. P., and A. Bradley.** 1990. The Wnt-1 (int-1) proto-oncogene is required for development of a large region of the mouse brain. Cell **62:**1073–1085.
53. **McMahon, A. P., A. L. Joyner, A. Bradley, and J. A. McMahon.** 1992. The midbrain-hindbrain phenotype of Wnt-1^{-}/Wnt-1^{-} mice results from stepwise deletion of engrailed-expressing cells by 9.5 days postcoitum. Cell **69:**581–595.
54. **Meznikova, M., N. Erdmann, R. Allsopp, and L. A. Harrington.** 2009. Telomerase reverse transcriptase-dependent telomere equilibration mitigates tissue dysfunction in mTert heterozygotes. Dis. Model Mech. **2:**620–626.
55. **Millar, S. E.** 2009. Cell biology: the not-so-odd couple. Nature **460:**44–45.
56. **Miller, C., and D. A. Sassoon.** 1998. Wnt-7a maintains appropriate uterine patterning during the development of the mouse female reproductive tract. Development **125:**3201–3211.
57. **Mitchell, J. R., E. Wood, and K. Collins.** 1999. A telomerase component is defective in the human disease dyskeratosis congenita. Nature **402:**551–555.
58. **Molenaar, M., et al.** 1996. XTcf-3 transcription factor mediates beta-catenin-induced axis formation in Xenopus embryos. Cell **86:**391–399.
59. **Monkley, S. J., S. J. Delaney, D. J. Pennisi, J. H. Christiansen, and B. J. Wainwright.** 1996. Targeted disruption of the Wnt2 gene results in placentation defects. Development **122:**3343–3353.
60. **Park, J. I., et al.** 2009. Telomerase modulates Wnt signalling by association with target gene chromatin. Nature **460:**66–72.
61. **Parr, B. A., and A. P. McMahon.** 1995. Dorsalizing signal Wnt-7a required for normal polarity of D-V and A-P axes of mouse limb. Nature **374:**350–353.
62. **Parry, E. M., J. M. Alder, J. X. Qi, J.-L. Chen, and M. Armanios.** 24 March 2011. Syndrome complex of bone marrow failure and pulmonary fibrosis predicts germline defects in telomerase. Blood [Epub ahead of print.] doi: 10.1182/blood-2010-11-322149.
63. **Poon, S. S. S., and P. M. Lansdorp.** 1 November 2001, posting date. Quantitative fluorescence in situ hybridization (Q-FISH). Curr. Protoc. Cell Biol. **Chapter 18:**Unit 18.14. doi:10.1002/0471143030.cb1804s12.
64. **Rudolph, K. L., et al.** 1999. Longevity, stress response, and cancer in aging telomerase-deficient mice. Cell **96:**701–712.
65. **Sarin, K. Y., et al.** 2005. Conditional telomerase induction causes proliferation of hair follicle stem cells. Nature **436:**1048–1052.
66. **Smith, L. L., H. A. Coller, and J. M. Roberts.** 2003. Telomerase modulates expression of growth-controlling genes and enhances cell proliferation. Nat. Cell Biol. **5:**474–479.
67. **Smogorzewska, A., and T. de Lange.** 2004. Regulation of telomerase by telomeric proteins. Annu. Rev. Biochem. **73:**177–208.
68. **Stark, K., S. Vainio, G. Vassileva, and A. P. McMahon.** 1994. Epithelial transformation of metanephric mesenchyme in the developing kidney regulated by Wnt-4. Nature **372:**679–683.
69. **Thomas, K. R., T. S. Musci, P. E. Neumann, and M. R. Capecchi.** 1991. Swaying is a mutant allele of the proto-oncogene Wnt-1. Cell **67:**969–976.
70. **Tsakiri, K. D., et al.** 2007. Adult-onset pulmonary fibrosis caused by mutations in telomerase. Proc. Natl. Acad. Sci. U. S. A. **104:**7552–7557.
71. **Vidal-Cardenas, S. L., and C. W. Greider.** 2010. Comparing effects of mTR and mTERT deletion on gene expression and DNA damage response: a critical examination of telomere length maintenance-independent roles of telomerase. Nucleic Acids Res. **38:**60–71.
72. **Vulliamy, T., et al.** 2001. The RNA component of telomerase is mutated in autosomal dominant dyskeratosis congenita. Nature **413:**432–435.
73. **Vulliamy, T., et al.** 2004. Disease anticipation is associated with progressive telomere shortening in families with dyskeratosis congenita due to mutations in TERC. Nat. Genet. **36:**447–449.
74. **Vulliamy, T. J., and I. Dokal.** 2008. Dyskeratosis congenita: the diverse clinical presentation of mutations in the telomerase complex. Biochimie **90:**122–130.
75. **Walne, A. J., and I. Dokal.** 2009. Advances in the understanding of dyskeratosis congenita. Br. J. Haematol. **145:**164–172.
76. **Wong, K. K., et al.** 2000. Telomere dysfunction impairs DNA repair and enhances sensitivity to ionizing radiation. Nat. Genet. **26:**85–88.
77. **Yamaguchi, H.** 2007. Mutations of telomerase complex genes linked to bone marrow failures. J. Nippon Med. Sch. **74:**202–209.
78. **Yamaguchi, H., et al.** 2003. Mutations of the human telomerase RNA gene (TERC) in aplastic anemia and myelodysplastic syndrome. Blood **102:**916–918.
79. **Yamaguchi, H., et al.** 2005. Mutations in TERT, the gene for telomerase reverse transcriptase, in aplastic anemia. N. Engl. J. Med. **352:**1413–1424.
80. **Yamaguchi, T. P., A. Bradley, A. P. McMahon, and S. Jones.** 1999. A Wnt5a pathway underlies outgrowth of multiple structures in the vertebrate embryo. Development **126:**1211–1223.
81. **Yuan, X., et al.** 1999. Presence of telomeric G-strand tails in the telomerase catalytic subunit TERT KO mice. Genes Cells **4:**563–572.
82. **Zhang, J. Z.** 2003. Overexpression analysis of plant transcription factors. Curr. Opin. Plant Biol. **6:**430–440.